Energy Band and Wave Modes for a Super-Cell of a Defected Periodic Viaduct

Cheng-Yong He[#1], Li Lei[#2], Jian-Fei Lu[*]

[#]*Department of Civil Engineering and Mechanics, Jiangsu University, Zhenjiang 212013, China*

Abstract-- **In this study, the influence of different defects on the energy bands of a super cell of a defected periodic viaduct (DPV) when considering the pile-soil-structure interaction is investigated. By using the coupled boundary element method (BEM) model for the piles supporting the superstructure of the DPV, the compliances of the pile foundations are obtained. By using the compliances of the piles and the transfer matrices for the beams and piers, the transfer matrix for each span of the DPV is determined. The eigenvalue equation for the super cell of the DPV can be developed by using the transfer matrices for the spans of the super cell and the Bloch theorem, the solution of which yields the energy bands for the super-cell. Numerical results show that the defected span may give rise to the defect state for the super cell of the DPV.**

Keywords-- **Defected periodic viaduct (DPV); super-cell method; the boundary element method (BEM); the pile-soil-structure interaction.**

I. INTRODUCTION

As viaduct can be used to resolve the settlement of soft soil bases effectively, they are now widely used in the high speed railways. For convenience, viaducts in normal sections are usually designed to consist of identical spans, so they can be simplified as periodic structures. For periodic viaducts with super long spans, they can be further idealized as infinite periodic structures. However, due to practical requirements, some spans of the viaduct are not identical with the standard span, making the viaduct defected. In this study, the spans different from the standard span are referred to as defected spans, and a periodic viaduct containing defected spans is called a defected periodic viaduct (DPV) [1-2].

Brillouin [3], Mead [4-6] and Lin [7] analyzed wave propagation in common periodic structures, and their researches show that waves in periodic structures are quite different from those in continuum media: the passband and stopband characteristic of the waves usually occurs in a periodic structure. It is noted that the behaviors of waves in a defected periodic structure is even more complicated than those in common periodic structures. By numerical simulation, Wu [8-9] found that in a defected periodic continuum medium, a sharp peak occurs around the defected cell in the defect state mode. Up to now, there have been some studies concerning defected periodic beams. Lin & Yang [10-11] analyzed a periodic beam with random defects. Mead [12-14] investigated the free waves propagating along a periodic beam with a single defect. Based on the researches of Mead, Bansal [15] investigated periodic beams with multiple defects and found that the influence of defects on the wave propagating along a periodic beam is significant because of

wave localization. Furthermore, Mead & Bansal [16] studied the response of a mono-coupled periodic beam with a single defect to a convected loading, finding that wave motion in the defected periodic beam may be localized around the defect. In summary, the presence of defected spans in a periodic beam may alter the wave characteristic of the structure, causing the localization of wave motion around the defects.

Existing studies concerning the beam-type periodic structure with defects are usually limited to continuous periodic beams, wherein beams are supposed to be continuous and supported by various periodically placed supporters. Since the viaduct considered in this study consists of a series of separate beams, piers and supporting piles, it is thus unreasonable to simplify the viaduct as a continuous beam. Therefore, this paper will develop the super-cell method for the DPV and the defect states associated with some defects are investigated.

II. THE GENERAL STATEMENT AND APPROCH FOR THE PROBLEM IN THIS STUDY

Generally, a practical viaduct may be decomposed into two parts: substructure and superstructure. For simplicity, it is supposed in this study that each span of the viaduct only contains one pier and each pier of the viaduct is supported by an effective pile foundation. Also, the piers and piles are assumed to be rigidly connected. Thus, the substructure of the viaduct is simplified as a pile row embedded in the half-space soil as shown in Figure 1. Also, each span of the superstructure of the periodic viaduct is simplified as a unit composed of a pier, two composite beams (left and right beams) and three linking springs, that is, the beam-beam, left and right beam-pier springs, respectively (Figure 1). The three springs form the beam-beam-pier (BBP) junction for each span of the viaduct.
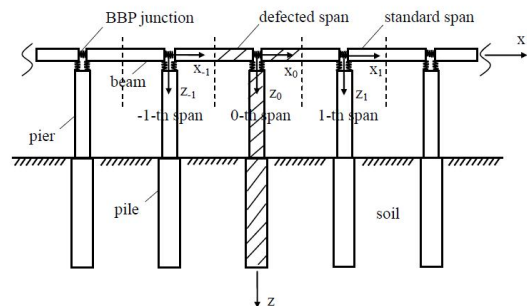

Fig. 1 Illustration for an infinite DPV

Generally, when a periodic viaduct is undergoing vibration, both the in-plane and out-of-plane vibrations may occur. Note that: the plane here is referred to as the plane passing through

the viaduct, namely, the *xoz* plane in Figure 1. Since the half-space soil, piles and super-structure of the viaduct in this study are assumed to be material and geometrically linear, the in-plane and out-of-plane vibrations of the viaduct are thus independent and can be investigated independently. In this paper, we only investigate the defect state for the DPV undergoing in-plane vibration.

III. A COUPLED BEM MODEL FOR THE PILE-SOIL INTERACTION PROBLEM

To account for the coupling between the superstructure of the viaduct and the pile foundations, the pile-soil interaction problem should be solved first. The separations between the neighboring effective piles are assumed to be large enough such that the interaction between the piles can be neglected. Hence, the multiple pile-soil interaction problem is simplified as a single pile-soil interaction problem. In this section, a coupled BEM model for a single pile embedded in the half-space soil will be developed, whereby the compliances of the pile foundation can be determined.

A. Boundary Integral Equation for an Elastic Medium

In this study, the pile and half-space soil are treated as the elastic medium. The equation of motion for an elastic medium in the frequency domain has the following expression [17]

$$\mu u_{i,jj} + (\lambda + \mu)u_{j,ji} = -\rho\omega^2 u_i \qquad (1)$$

in which λ and μ are the Lame constants of the elastic medium; μ_i is the displacement; ρ is the density; ω is the angular frequency. Note that the frequency domain variable and time domain variable are related to each other by the Fourier transform for time and frequency. In this study, the Fourier transform with respect to time and frequency is defined as follows [18]

$$\hat{f}(\omega) = \int_{-\infty}^{+\infty} f(t)e^{-i\omega t}dt, \quad f(t) = \frac{1}{2\pi}\int_{-\infty}^{+\infty} \hat{f}(\omega)e^{i\omega t}d\omega \qquad (2)$$

where *t* represent the time; a variable with a caret denotes the frequency domain variables. As this study is restricted to the frequency domain analysis of the defected viaduct, for brevity, the caret denoting the frequency domain variable is dropped for all the frequency domain variables. The constitutive relation for the elastic medium is as follows [17]

$$\sigma_{ij} = 2\mu\varepsilon_{ij} + \lambda\delta_{ij}e \qquad (3)$$

in which σ_{ij} and ε_{ij} are the stress and strain components for the elastic medium, respectively; *e* and δ_{ij} denotes the bulk strain and the Kronecker delta, respectively. Based on the dynamic reciprocal theorem, the frequency domain boundary integral equation for the elastic medium is obtained as follows [19]

$$c_{ij}u_j(\mathbf{x}) = \int_{\Gamma}[U_{ij}^{(G)}(\mathbf{x},\mathbf{y})t_j(\mathbf{y}) - T_{ij}^{(G)}(\mathbf{x},\mathbf{y})u_j(\mathbf{y})]d\Gamma(\mathbf{y}) \qquad (4)$$

in which $U_{ij}^{(G)}$ and $T_{ij}^{(G)}$ are the Green's functions for the elastic medium and given in Appendix; u_j and t_j are the displacements and tractions along the boundary of the elastic medium; c_{ij} is the coefficients for the boundary and Γ denotes the boundary of the elastic medium.

B. Derivation of the Coupled BEM Model for the Pile and Half-Space Soil

In this section, according to the boundary integral equations for the elastic medium, boundary element formulations for the pile and half-space soil are established, respectively. By using the boundary element formulations as well as the boundary conditions and continuity conditions at the pile-soil interface, a coupled BEM model for the pile and half-space soil will be developed. As shown in Figure 2, for a pile embedded in a half-space soil, the whole boundary of the pile-soil system consists of three parts, that is, the interface between the pile and half-space soil (Γ_1), the boundary of the pile top (Γ_2), and the surface of the half-space soil (Γ_3), respectively. The boundary of the pile consists of Γ_1 and Γ_2, respectively and the boundary of the half-space soil is composed of Γ_1 and Γ_3, respectively.
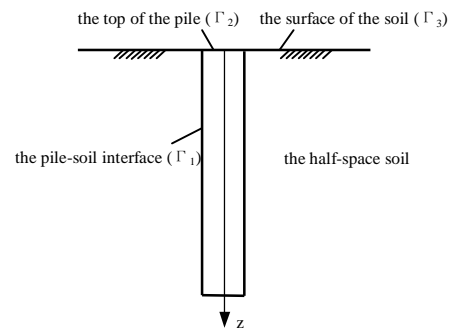

Fig. 2 The illustration for a pile embedded in an elastic half-space

The frequency domain integral equations for the pile and half-space soil can be discretized if suitable numbers of boundary elements are used to discretize the corresponding boundaries. Suppose that the boundaries of the pile and half-space soil are discretized by the same type of iso-parametric element, each boundary element containing N_{nd} nodes. Thus, for a point **x** inside the j-th element, the following interpolation formulae hold [20]

$$\mathbf{x}^{(j)}(\xi,\eta) = \sum_{n=1}^{N_{nd}} N_n(\xi,\eta)\mathbf{x}_n^{(j)}, \quad \mathbf{u}^{(j)}(\kappa,\mathbf{x}^{(j)}) = \sum_{n=1}^{N_{nd}} N_n(\xi,\eta)\mathbf{u}_n^{(j)}(\kappa),$$

$$\mathbf{t}^{(j)}(\kappa,\mathbf{x}^{(j)}) = \sum_{n=1}^{N_{nd}} N_n(\xi,\eta)\mathbf{t}_n^{(j)}(\kappa) \qquad (5)$$

where the superscript j denotes the element number; *n* is the local node number; ξ, η are the intrinsic coordinates corresponding to the point $\mathbf{x}^{(j)}$; $\mathbf{x}_n^{(j)}$ is the n-th node coordinate of the j-th element in the global coordinate system;

$N_n(\xi, \eta)$ is the n-th shape function; $\mathbf{u}_n^{(j)}(\kappa)$ and $\mathbf{t}_n^{(j)}(\kappa)$ represent the displacement and traction vectors at the n-th node of the j-th element.

Using equation (5) in the boundary integral equation for the pile and integrating the shape function kernel products over all boundary elements for the pile, the boundary element formulation for the pile is obtained as follows

$$\mathbf{H}^{(p)}\mathbf{u}^{(p)} = \mathbf{G}^{(p)}\mathbf{t}^{(p)} \qquad (6)$$

in which the superscript p denotes the pile; $\mathbf{G}^{(p)}$ and $\mathbf{H}^{(p)}$ are the coefficient matrices obtained by integrating shape function kernel products over all boundary elements of the pile; $\mathbf{u}^{(p)}$ and $\mathbf{t}^{(p)}$ are the generalized displacement and traction vectors of the nodes of the boundary elements of the pile. Dividing $\mathbf{u}^{(p)}$ and $\mathbf{t}^{(p)}$ into two parts corresponding to Γ_1 and Γ_2, respectively, and partitioning the coefficient matrices $\mathbf{G}^{(p)}$ and $\mathbf{H}^{(p)}$ accordingly, equation (6) is rewritten as follows

$$\left[\mathbf{H}_1^{(p)}\ \mathbf{H}_2^{(p)}\right]\begin{Bmatrix}\mathbf{u}_1^{(p)}\\ \mathbf{u}_2^{(p)}\end{Bmatrix} = \left[\mathbf{G}_1^{(p)}\ \mathbf{G}_2^{(p)}\right]\begin{Bmatrix}\mathbf{t}_1^{(p)}\\ \mathbf{t}_2^{(p)}\end{Bmatrix} \qquad (7)$$

in which the subscripts 1 and 2 represent the boundaries Γ_1 and Γ_2 of the pile, respectively; $\mathbf{u}_j^{(p)}, \mathbf{t}_j^{(p)}, j = 1, 2$ denote the generalized displacement and traction vectors for the boundaries $\Gamma_j, j = 1, 2$ of the pile, respectively; $\mathbf{H}_1^{(p)}, \mathbf{H}_2^{(p)}$ and $\mathbf{G}_1^{(p)}, \mathbf{G}_2^{(p)}$ are the sub-matrices of the coefficient matrices $\mathbf{H}^{(p)}$ and $\mathbf{G}^{(p)}$ of the pile, corresponding to the boundaries Γ_1 and Γ_2, respectively.

Likewise, applying equation (5) to the boudary integral equaiton of the half-space soil and implementing the similar BEM procedure, the boundary element formulation for the half-space soil is derived as follows

$$\mathbf{H}^{(s)}\mathbf{u}^{(s)} = \mathbf{G}^{(s)}\mathbf{t}^{(s)} \qquad (8)$$

in which the superscript s denotes the half-space soil; $\mathbf{u}^{(s)}$ and $\mathbf{t}^{(s)}$ are the generalized displacement and traction vectors of the nodes of the boundary elements of the half-space soil; $\mathbf{G}^{(s)}$ and $\mathbf{H}^{(s)}$ are the coefficient matrices. Analogously, partitioning the coefficient matrices as well as the displacement and traction vectors in equation (8) corresponding to the boundaries Γ_1 and Γ_3 of the half-space soil, the boundary element formulation (8) for the half-space soil is reformulated as follows

$$\left[\mathbf{H}_1^{(s)}\ \mathbf{H}_3^{(s)}\right]\begin{Bmatrix}\mathbf{u}_1^{(s)}\\ \mathbf{u}_3^{(s)}\end{Bmatrix} = \left[\mathbf{G}_1^{(s)}\ \mathbf{G}_3^{(s)}\right]\begin{Bmatrix}\mathbf{t}_1^{(s)}\\ \mathbf{t}_3^{(s)}\end{Bmatrix} \qquad (9)$$

in which $\mathbf{u}_j^{(s)}$ and $\mathbf{t}_j^{(s)}, j = 1, 3$ denote the generalized displacement and traction vectors for the boundaries $\Gamma_j, j = 1, 3$ of the half-space soil, respectively; $\mathbf{H}_1^{(s)}, \mathbf{H}_3^{(s)}$, $\mathbf{G}_1^{(s)}$ and $\mathbf{G}_3^{(s)}$ are the sub-matrices of the coefficient matrices of the half-space soil for the boundaries Γ_1 and Γ_3 of the half-space soil, respectively.

At the interface Γ_1, the pile and soil should satisfy displacement and traction continuity conditions. The boundary conditions at the top of the pile (Γ_2) are determined by the loads acting on the top of the pile. Thus, $\mathbf{t}_2^{(p)}$ in equation (7) is assumed to be known *a priori*. Moreover, at the surface Γ_3, the half-space soil is supposed to be stress free. As a result, the following continuity conditions and boundary condition should be fulfilled along the interface Γ_1 and the boundary Γ_3, respectively

$$\mathbf{u}_1^{(p)} = \mathbf{u}_1^{(s)}, \quad \mathbf{t}_1^{(p)} = -\mathbf{t}_1^{(s)}, \quad \mathbf{t}_3^{(s)} = \mathbf{0} \qquad (10)$$

By using the boundary element formulations for the pile and soil as given by equations (7) and (9) as well as the continuity conditions and boundary condition in equation (10), a coupled BEM model for the pile-soil system is obtained as follows

$$\begin{bmatrix}\mathbf{H}_1^{(p)} & -\mathbf{G}_1^{(p)} & \mathbf{H}_2^{(p)} & \mathbf{0}\\ \mathbf{H}_1^{(s)} & \mathbf{G}_1^{(s)} & \mathbf{0} & \mathbf{H}_3^{(s)}\end{bmatrix}\begin{bmatrix}\mathbf{u}_1^{(p)} & \mathbf{t}_1^{(p)} & \mathbf{u}_2^{(p)} & \mathbf{u}_3^{(s)}\end{bmatrix}^T$$
$$= \begin{bmatrix}\mathbf{G}_2^{(p)}\mathbf{t}_2^p\\ \mathbf{0}\end{bmatrix} \qquad (11)$$

IV. ANALYSIS OF THE SUPER STRUCTURE OF THE DPV IN THE WAVENUMBER DOMAIN

In this section, the governing equations for the piers and beams of the viaduct undergoing in-plane vibration will be outlined.

A. The Transfer Matrices for the Piers and Beams

The in-plane vibration of the periodic viaduct will involve the longitudinal and in-plane flexural vibrations of the piers and beams. As the piers are treated as 1-D rods and beams, their transfer matrices can be derived by the conventional vibration theories for a rod and beam undergoing axial and flexural vibrations, respectively. For simplicity, the vibration of the beams in this study is described by the Bernoulli-Euler beam theory [17]. Thus, the frequency-wavenumber domain equations of motion for the longitudinal and in-plane flexural vibrations of the pier in the n-th span of the periodic viaduct are given as follows [17]

$$E_d \frac{d^2 u_d^{(n)}(z^{(e)})}{dz^{(e)2}} + \rho_d \omega^2 u_d^{(n)}(z^{(e)}) = 0 ,$$

$$E_d I_d \frac{d^4 v_d^{(n)}(z^{(e)})}{dz^{(e)4}} - \rho_d A_d \omega^2 v_d^{(n)}(z^{(e)}) = 0 \qquad (12)$$

where the subscript d denotes the pier; ρ_d and E_d are the density and elastic modulus of the pier; A_d and I_d are the cross section area and second moment of the cross section of the pier; $u_d^{(n)}, v_d^{(n)}$ are the axial and transverse displacements, respectively; $z^{(e)}$ denotes the local vertical coordinate of the cross-section of the pier.

For the internal forces of the pier, the following relations hold [17]

$$N_d^{(n)}(z^{(e)}) = E_d A_d \frac{du_d^{(n)}(z^{(e)})}{dz^{(e)}} ,$$

$$M_d^{(n)}(z^{(e)}) = -E_d I_d v_d^{(n)"}(z^{(e)}) ,$$

$$Q_d^{(n)}(z^{(e)}) = -\frac{dM_d^{(n)}(z^{(e)})}{dz^{(e)}} \qquad (13)$$

where $N_d^{(n)}$, $Q_d^{(n)}$ and $M_d^{(n)}$ are the axial, shear force and moment of the cross-section. For the pier of the n-th span undergoing in-plane vibration, the displacement, internal force vectors and state vector for an arbitrary cross-section are defined as follows

$$\mathbf{q}_d^{(n)}(z^{(e)}) = \{u_d^{(n)}(z^{(e)}), v_d^{(n)}(z^{(e)}), \theta_d^{(n)}(z^{(e)})\}^T ,$$

$$\mathbf{f}_d^{(n)}(z^{(e)}) = \{N_d^{(n)}(z^{(e)}), Q_d^{(n)}(z^{(e)}), M_d^{(n)}(z^{(e)})\}^T ,$$

$$\boldsymbol{\psi}_d^{(n)}(z^{(e)}) = \{\mathbf{q}_d^{(n)T}(z^{(e)}), \mathbf{f}_d^{(n)T}(z^{(e)})\}^T \qquad (14)$$

in which $\theta_d^{(n)}$ is the rotation angle of the cross-section $z^{(e)}$ of the n-th pier; $\mathbf{q}_d^{(n)}$, $\mathbf{f}_d^{(n)}$ and $\boldsymbol{\psi}_d^{(n)}$ represent the displacement and internal force vectors as well as the state vector, respectively. By using equations (12), (13) and (14), the transfer matrix for the pier undergoing in-plane vibration can be derived.

Likewise, the frequency-wavenumber domain equations of motion for the longitudinal and in-plane flexural vibrations of the beams of the n-th span have the following expressions

$$E_b \frac{d^2 u_b^{(n)}(x^{(e)})}{dx^{(e)2}} + \rho_b \omega^2 u_b^{(n)}(x^{(e)}) = 0 ,$$

$$E_b I_b \frac{d^4 v_b^{(n)}(x^{(e)})}{dx^{(e)4}} - \rho_b A_b \omega^2 v_b^{(n)}(x^{(e)}) = 0 \qquad (15)$$

where the subscript b denotes the beams; ρ_b and E_b are the density and elastic modulus of the beams; A_b and I_b are the cross section area and second moment of the cross section of the beams; $u_b^{(n)}$, $v_b^{(n)}$ are the axial and transverse displacements, respectively; $x^{(e)}$ represents the local longitudinal coordinate for the cross-section of the beams.

For the internal forces of the beams, the following relations hold

$$N_b^{(n)}(x^{(e)}) = E_b A_b \frac{du_b^{(n)}(x^{(e)})}{dx^{(e)}} ,$$

$$M_b^{(n)}(x^{(e)}) = -E_b I_b v_b^{(n)"}(x^{(e)}) ,$$

$$Q_b^{(n)}(x^{(e)}) = \frac{dM_b^{(n)}(x^{(e)})}{dx^{(e)}} \qquad (16)$$

where $N_b^{(n)}$, $Q_b^{(n)}$ and $M_b^{(n)}$ are the axial, shear forces and moment of the cross-section. For the beams of the n-th span undergoing in-plane vibration, the displacement and internal force vectors and the state vector at the cross-section $x^{(e)}$ are defined as follows

$$\mathbf{q}_b^{(n)}(x^{(e)}) = \{u_b^{(n)}(x^{(e)}), v_b^{(n)}(x^{(e)}), \theta_b^{(n)}(x^{(e)})\}^T ,$$

$$\mathbf{f}_b^{(n)}(x^{(e)}) = \{N_b^{(n)}(x^{(e)}), Q_b^{(n)}(x^{(e)}), M_b^{(n)}(x^{(e)})\}^T ,$$

$$\boldsymbol{\psi}_b^{(n)}(x^{(e)}) = \{\mathbf{q}_b^{(n)T}(x^{(e)}), \mathbf{f}_b^{(n)T}(x^{(e)})\}^T \qquad (17)$$

in which $\theta_b^{(n)}$ is the rotation angle of the cross-section $x^{(e)}$ of the beams; $\mathbf{q}_b^{(n)}$, $\mathbf{f}_b^{(n)}$ and $\boldsymbol{\psi}_b^{(n)}$ represent the displacement and internal force vectors as well as the state vector for the cross-section of the beams, respectively. By using equations (15)-(17), the transfer matrix for the beams undergoing in-plane vibration can be derived.

B. Coupling between the Pile-Soil System and the Super Structure

The displacement and force vectors of the n-th pile top are related to each other by the compliances of the pile, namely

$$\mathbf{q}_p^{(n)}(0) = \mathbf{C}_p^{(n)} \mathbf{f}_p^{(n)}(0) ,$$

$$\mathbf{q}_p^{(n)}(0) = \{u_p^{(n)}(0), v_p^{(n)}(0), \theta_p^{(n)}(0)\}^T ,$$

$$\mathbf{f}_p^{(n)}(0) = \{N_p^{(n)}(0), Q_p^{(n)}(0), M_p^{(n)}(0)\}^T \qquad (18)$$

where $\mathbf{C}_p^{(n)}$ is the 3×3 compliance matrix for the pile, which can be obtained using the aforementioned BEM model for the pile-soil system; $\mathbf{q}_p^{(n)}(0)$ and $\mathbf{f}_p^{(n)}(0)$ are displacement and internal force vectors at the top of the pile.

As noted above, it is assumed that the pile and pier are rigidly connected, the displacement and force vectors at the bottom of the n-th pier are equal to those at the n-th pile top, namely

$$\mathbf{q}_d^{(n)}(L_d^{(n)}) = \mathbf{q}_p^{(n)}(0) , \quad \mathbf{f}_d^{(n)}(L_d^{(n)}) = \mathbf{f}_p^{(n)}(0) \qquad (19)$$

in which $L_d^{(n)}$ is the height of the n-th pier. By using equation

(18) and (19), one has the following relation for the displacement and force vectors at the bottom of the n-th pier

$$\mathbf{q}_d^{(n)}(L_d^{(n)}) = \mathbf{C}_p^{(n)}\mathbf{f}_d^{(n)}(L_d^{(n)}) \qquad (20)$$

Then, the relation between the state vectors at the top and bottom of the n-th pier is obtained as follows

$$\begin{Bmatrix} \mathbf{C}_p^{(n)}\mathbf{f}_d^{(n)}(L_d^{(n)}) \\ \mathbf{f}_d^{(n)}(L_d^{(n)}) \end{Bmatrix} = \begin{bmatrix} \mathbf{T}_{qq}^{(d)}(L_d^{(n)}) & \mathbf{T}_{qf}^{(d)}(L_d^{(n)}) \\ \mathbf{T}_{fq}^{(d)}(L_d^{(n)}) & \mathbf{T}_{ff}^{(d)}(L_d^{(n)}) \end{bmatrix} \begin{Bmatrix} \mathbf{q}_d^{(n)}(0_+) \\ \mathbf{f}_d^{(n)}(0_+) \end{Bmatrix} \qquad (21)$$

Using equation(21), the relation between the displacement and force vectors at the top of the n-th pier is obtained as follows

$$\mathbf{q}_d^{(n)}(0) = \mathbf{C}_d^{(n)}(\kappa)\mathbf{f}_d^{(n)}(0) ,$$

$$\mathbf{C}_d^{(n)} = [\mathbf{T}_{qq}^{(d)}(L_d^{(n)}) - \mathbf{C}_p\mathbf{T}_{fq}^{(d)}(L_d^{(n)})]^{-1}[\mathbf{C}_p\mathbf{T}_{ff}^{(d)}(L_d^{(n)}) - \mathbf{T}_{qf}^{(d)}(L_d^{(n)})] \qquad (22)$$

By using the equilibrium conditions at the junction [21], the relation between the state vectors of the beam sections to the right and left of the n-th junction is obtained as follows

$$\begin{Bmatrix} \mathbf{q}_b^{(n)}(0_+) \\ \mathbf{f}_b^{(n)}(0_+) \end{Bmatrix} = \mathbf{S}_J^{(n)} \begin{Bmatrix} \mathbf{q}_b^{(n)}(0_-) \\ \mathbf{f}_b^{(n)}(0_-) \end{Bmatrix}, \quad \mathbf{S}_J^{(n)} = \mathbf{A}^{(n)-1}\mathbf{B}^{(n)},$$

$$\mathbf{A}^{(n)} = \begin{bmatrix} \mathbf{J}_{lr}^{(n)} & \mathbf{J}_{ld}^{(n)}\mathbf{E}_r^{(n)(b)} \\ \mathbf{J}_{rr}^{(n)} & \mathbf{J}_{rd}^{(n)}\mathbf{E}_r^{(n)(b)} - \mathbf{I}_{3\times3} \end{bmatrix}, \quad \mathbf{B}^{(n)} = \begin{bmatrix} -\mathbf{J}_{ll}^{(n)} & \mathbf{I}_{3\times3} - \mathbf{J}_{ld}^{(n)}\mathbf{E}_l^{(n)(b)} \\ -\mathbf{J}_{rl}^{(n)} & -\mathbf{J}_{rd}^{(n)}\mathbf{E}_l^{(n)(b)} \end{bmatrix},$$

$$\mathbf{E}_l^{(n)(b)} = \mathbf{C}_d^{(n)}\mathbf{E}_l^{(a)}, \mathbf{E}_r^{(n)(b)} = \mathbf{C}_d^{(n)}\mathbf{E}_r^{(a)} \qquad (23)$$

in which the matrix $\mathbf{S}_J^{(n)}$ is referred to as the junction transfer matrix at the n-th BBP junction, and the representations for $\mathbf{E}_l^{(a)}, \mathbf{E}_r^{(a)}$, $\mathbf{J}_{ll}^{(n)}, \mathbf{J}_{lr}^{(n)}, \mathbf{J}_{ld}^{(n)}, \mathbf{J}_{rl}^{(n)}, \mathbf{J}_{rr}^{(n)}$ and $\mathbf{J}_{rd}^{(n)}$ are given in [21]. It is noted that for a periodic viaduct, the junction transfer matrix is identical for all the BBP junctions. By using equation (23) and the transfer matrices for the beams of the n-th span, one has the following relation for the state vectors at the right and left ends of the n-th span

$$\boldsymbol{\psi}_b^{(n)}(x_R^{(e)}) = \mathbf{T}_R^{(n)(b)}\mathbf{S}_J^{(n)}\mathbf{T}_L^{(n)(b)}\boldsymbol{\psi}_b^{(n)}(x_L^{(e)}) \qquad (24)$$

where $\mathbf{T}_L^{(n)(b)}$ and $\mathbf{T}_R^{(n)(b)}$ are the transfer matrices for the left and right beams; $\boldsymbol{\psi}_b^{(n)}(x_L^{(e)})$ and $\boldsymbol{\psi}_b^{(n)}(x_R^{(e)})$ are the state vectors for the left and right ends of the n-th span, respectively; $x_L^{(e)}$ and $x_R^{(e)}$ denote the x-coordinates of the left and right ends of the n-th span in the local coordinate system (Figure 1). Note that for the standard span, the transfer matrices for the left and right beams $\mathbf{T}_L^{(n)(b)}$ and $\mathbf{T}_R^{(n)(b)}$ are identical and given by

$$\mathbf{T}_L^{(b)} = \mathbf{T}_R^{(b)} = \mathbf{T}^{(b)}(\frac{L}{2}) \qquad (25)$$

where L is the length of the standard span of the viaduct; $\mathbf{T}^{(b)}(L/2)$ is the transfer matrix for the left and right beams .

V. THE EIGHEVALUE EQUATION FOR THE SUPER-CELL OF THE DPV

A periodic structure with defects usually displays characteristics associated with defect state [1]. Furthermore, the defect state characteristics of a periodic structure are usually relevant to its dynamic response. Consequently, to fully understand the dynamic response of a defected viaduct, it is necessary to investigate the defect state of the defected viaduct. In this section, by means of the super-cell method and transfer matrix method, the eigenvalue equation for a super-cell of the defected viaduct will be derived, whereby the defect state of the defected viaduct can be identified.

To investigate the defect state of the DPV, it is necessary to define a super-cell for the DPV. The super-cell of the viaduct should contain the defected span and also it should contain sufficient number of spans of the viaduct to make the responses of the super-cell associated with the defect state mode negligible at the edges of the super-cell. It is supposed that the super-cell contains $2N+1$ spans of the viaduct, the central span (the 0th span) being the defected span.

Equation (24) implies that the transfer matrix for standard and defected spans of the DPV has the following expressions

$$\mathbf{T}^{(s)} = \mathbf{T}^{(b)}(\frac{L}{2})\mathbf{S}_J\mathbf{T}^{(b)}(\frac{L}{2}), \quad \mathbf{T}^{(q)} = \mathbf{T}_R^{(0)(b)}\mathbf{S}_J^{(0)}\mathbf{T}_L^{(0)(b)} \qquad (26)$$

where the superscripts s and q denote the standard and defected spans of the viaduct, respectively; $\mathbf{S}_J$ denotes the junction transfer matrix for the standard span of the viaduct.

By using the transfer matrices for the standard and defected spans, the relation between the state vectors at the right and left ends of the super-cell is obtained as follows

$$\boldsymbol{\psi}_b^{(N)}(\frac{L}{2}) = \overbrace{\mathbf{T}^{(s)}\cdots\mathbf{T}^{(s)}}^{N} \mathbf{T}^{(q)} \overbrace{\mathbf{T}^{(s)}\cdots\mathbf{T}^{(s)}}^{N} \boldsymbol{\psi}_b^{(-N)}(-\frac{L}{2}) \qquad (27)$$

Using the Bloch theorem [22] and equation(27), the following eigenvalue equation is derived for the super-cell of the viaduct

$$[\overbrace{\mathbf{T}^{(s)}\cdots\mathbf{T}^{(s)}}^{N} \mathbf{T}^{(q)} \overbrace{\mathbf{T}^{(s)}\cdots\mathbf{T}^{(s)}}^{N} - e^{-i\kappa_s L_s}\mathbf{I}_{6\times6}]\boldsymbol{\psi}_b^{(-N)}(-\frac{L}{2}) = \mathbf{0} ,$$

$$L_S = 2NL + L_q \qquad (28)$$

in which κ_s denotes the wavenumbers for the characteristic waves of the super-cell; L_q and L_s are the lengths of the defected span and super-cell, respectively. Solution of equation (28) yields the energy bands of the super-cell, whereby the defect state of the super-cell of the DPV can be identified.
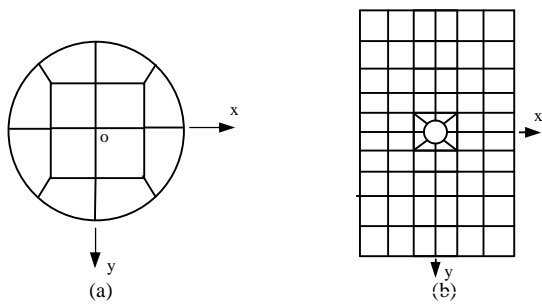
Fig. 3 The discretization schemes for the top and bottom of the piles as well as that for the surface of the half-space soil: (a) the discretization scheme for the piles; (b) the discretization scheme for the soil

VI. NUMERICAL RESULTS AND CORRESPONDING ANALYSIS

In this section, based on the proposed model, influence of the defected span on the defected periodic viaduct (DPV) will be investigated. In the numerical examples, the cross-sections of the piles and piers of the viaduct are assumed to be circular, while those of the beams are rectangular. The parameters for the soil, piles, piers, beams and spring stiffnesses of the standard span are given by Tables 1 and 2. For the defected span, the height of the pier is 15.0m, while other parameters are the same as those of the standard span.

The 2-D eight-node isoparametric boundary element [23] is used to discretize the boundaries of the pile and half-space soil. The top and bottom of the piles in both the standard span and defected span are discretized by twelve isoparametric boundary elements as shown in Figure 3 (a). The side of the pile is divided into fifteen segments evenly, and each segment is discretized by eight elements evenly. To truncate the surface of the half-space soil, the surface of the half-space soil is covered by some numbers of vertical and horizontal boundary element layers (Figure 3(b)). The numbers of vertical and horizontal boundary element layers used to cover the soil surface for different frequency ranges are given in Table 3.

Table 1 The geometrical and material parameters of the soil, piles, piers and beams

The shear modulus, Poisson's ratio and density for the half-space soil (μ_s, v_s, ρ_s)	2.0×10^7 Pa, 0.4, 2.0×10^3 kg/m^3
The length and radius of the piles (L_p, R_p)	15.0 m, 1.0 m
The Young's modulus, Poisson's ratio and density of the piles (E_p, v_p, ρ_p)	2.8×10^{10} Pa, 0.2, 2.4×10^3 kg/m^3
The height and radius of the piers (L_d, R_d)	10.0 m, 1.0 m
The Young's modulus, Poisson's ratio and density of the piers (E_d, v_d, ρ_d)	2.8×10^{10} Pa, 0.2, 3.0×10^3 kg/m^3
The length of each span of the periodic viaduct (L)	20.0 m
The width and depth of the rectangular cross-section of the beams (w_b, h_b)	3.0 m, 1.0 m
The Young's modulus, Poisson's ratio and density of the beams (E_b, v_b, ρ_b)	2.8×10^{10} Pa, 0.2, 3.6×10^3 kg/m^3
The calculated frequency range (f)	0~50 Hz

Table 2 The stiffnesses of the beam-beam, left beam-pier and right beam-pier springs of the standard span of the viaduct

The stiffnesses of the beam-beam spring for the in-plane vibration ($k_t^{(t)}$, $k_t^{(s)}$, $k_t^{(b)}$)	1.0×10^8 N/m, 1.0×10^8 N/m, 1.0×10^8 N.m/rad
The stiffnesses of the left beam-pier spring for the in-plane vibration ($k_l^{(t)}$, $k_l^{(s)}$, $k_l^{(b)}$)	1.0×10^8 N/m, 1.0×10^8 N/m, 1.0×10^7 N.m/rad
The stiffnesses of the right beam-pier spring for the in-plane vibration ($k_r^{(t)}$, $k_r^{(s)}$, $k_r^{(b)}$)	1.0×10^8 N/m, 1.0×10^8 N/m, 1.0×10^7 N.m/rad

Figure 4 shows the energy band of the third characteristic wave of the super-cell (consisting of twenty-three spans) of the DPV. It is noted that as the first and second characteristic waves are highly attenuative, only the energy bands for the third characteristic wave are presented. Figure 5 depicts the wave mode for the axial displacement at the left ends of different spans of the ordered and defected super-cell when the frequency is equal to 33.25Hz.

Table 3 The numbers of the vertical and horizontal boundary element layers used to discretize the surface of the half-space soil

Frequency range	BEM for a single pile (vertical $\times$ horizontal)
0-5Hz	18×18
5-20 Hz	16×16
20-40Hz	18×18
40-50 Hz	20×20

Figure 4 shows that 33.25Hz is located in a stopband of the ordered super-cell while in a passband of the defected super-cell, implying that frequency 33.25Hz is a defect state frequency for the defected super-cell of the DPV. Figure 5 indicates that, when the frequency coincides with the defect state frequency of the super cell, the axial displacement at the left end of the defected span is much larger than those of other spans, indicating that the axial displacement of the spans near the defected span is amplified significantly due to the presence of the defected span. Figure 5 also indicates that, for the ordered super cell, the axial displacement decays steadily along the spans and no amplification phenomenon occurs.
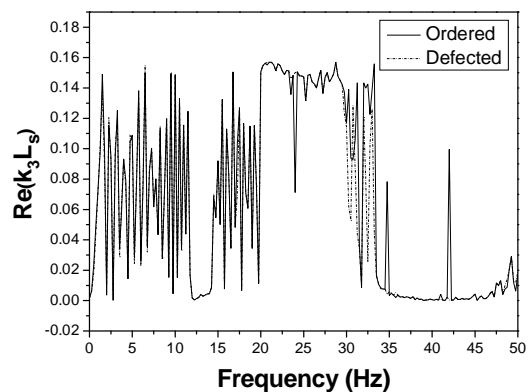
(a) The real part of the wavenumber
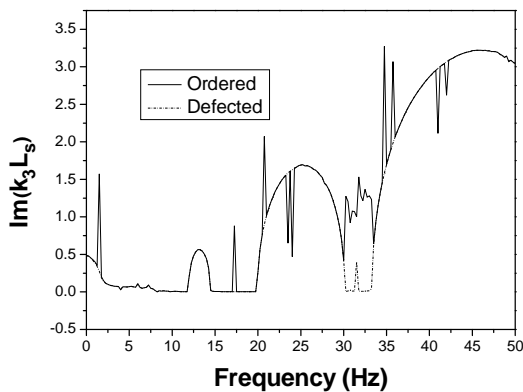
(b) The imaginary part of the wavenumber

Fig. 4 Influence of the defected span on the energy band of the third characteristic wave of the super-cell
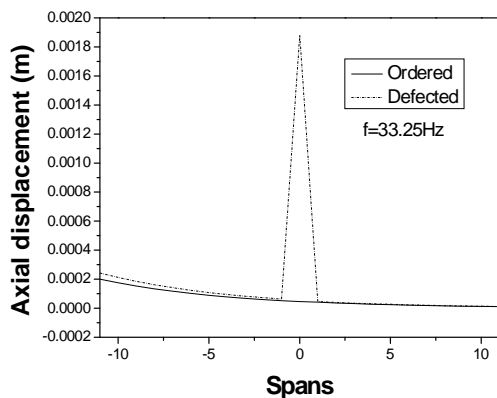

Fig. 5 The wave modes for the third characteristic wave of the ordered and defected super-cells when the frequency equals to 33.25Hz

VII. CONCLUSIONS

A model for the analysis of the influence of the defected span on the energy bands of the super cell for a DPV has been developed in this paper. Although the cross-section of the piers and beams are assumed to be uniform, the proposed approach is also applicable to the viaduct whose piers and beams have non-uniform cross-section if sub-division of piers and beams is performed. Alternatively, the finite element method can be used to discretize the non-uniform piers and beams and similar models can also be developed. Also, our model can be easily extended to deal with the DPV with several neighboring defected spans.

Numerical results show that, the defected span in an otherwise periodic viaduct will generate additional passband and confine the vibration of the DPV around the defected span, which makes the DPV more vulnerable when exposed to external loads.

REFERENCES

[1] M.M. Sigalas. Defect states of acoustic waves in two-dimensional lattice of solid cylinders, J Appl Phys. vol. 84, pp. 3026–3030, 1998.
[2] C.H. Hodges. Confinement of vibration by structure irregularity, J Sound Vib. vol. 82, pp. 411–424, 1982.
[3] L. Brillouin. Wave propagation in periodic structures, Dover Public Inc, New York. 1946.
[4] D.J. Mead. Free wave propagation in periodically supported infinite beams, J Sound Vib. vol. 11, pp. 181–197, 1970.
[5] D.J. Mead. Wave propagation in continuous periodic structures: Research contributions from Southampton, J Sound Vib. vol. 190, pp. 495–524, 1996.
[6] D.J. Mead. A general theory of harmonic wave propagation in linear periodic systems with multiple coupling, J Sound Vib. vol. 27, pp. 235–260, 1973.
[7] Y.K. Lin. Free vibrations of a continuous beam on elastic supports, Int J Mech Sci. vol.4, pp. 409–423, 1962.
[8] F.G. Wu, Z.Y. Liu, Y.Y. Liu. Stop gaps and single defect states of acoustic waves in two-dimensional lattice of liquid cylinders, Chin Phys Lett. vol. 18, pp. 785–787, 2001.
[9] F.G. Wu. Point defect states in two-dimensional phononic crystals, Phys Lett. vol. 292, pp. 198–202, 2001.
[10] Y.K. Lin, J.N. Yang. Free vibration of a disordered periodic beam, J Appl Mech. vol. 41, pp. 383–391, 1974.
[11] J.N. Yang, Y.K. Lin. Frequency response function of a disordered periodic beam, J Sound Vib. vol. 38, pp. 317–340, 1975.
[12] D.J. Mead. Wave propagation and natural modes in periodic systems: Mono-coupled systems, J Sound Vib. vol. 40, pp. 1–18, 1975.
[13] D.J. Mead. Wave propagation and natural modes in periodic systems: Multi-coupled systems, with and without damping, J Sound Vib. vol. 40, pp. 19–39, 1975.
[14] D.J. Mead, A.S. Bansal. Mono-coupled periodic systems with a single disorder: Free wave propagation, J Sound Vib. vol. 61, pp. 481–496, 1978.
[15] A.S. Bansal. Free wave motion in periodic systems with multiple disorders, J Sound Vib. vol. 60, pp. 389–400, 1978.
[16] D.J. Mead, A.S. Bansal, Mono-coupled periodic systems with a single disorder: Response to convected lodaings, J Sound Vib. vol. 61, pp. 497–515, 1978.
[17] K.F. Graff, Wave motion in elastic solids. Clarendon Press, Oxford, 1975.
[18] A.V. Oppenheim, A.S. Willsky, I.T. Young. Signals and systems, 2nd ed, Prentice Hall Englewood Cliffs, New Jersey, 1983.
[19] D. Clouteau, M.L. Elhabre, D. Aubry. Periodic BEM and FEM-BEM Coupling, COMPUT MECH. vol. 25, pp. 567–577, 2000.
[20] G.D. Manolis, D.E. Beskos. Boundary element methods in elastodynamics, Unwin Hyman, London, 1988.
[21] J.F. Lu, H.Y. Yuan. The sequence Fourier transform method for the analysis of a periodic viaduct subjected to non-uniform seismic. ACTA MECH, 2013.
[22] C. Kittel. Introduction to solid state physics, 7th ed, John Wiley & Sons, Inc, New York, 1996.
[23] G. Beer, L. Smith, C. Duenser. The boundary element method with programming: For engineers and scientists, Springer, Berlin, 2008.

APPENDIX-- THE FREQUENCY DOMAIN GREEN'S FUNCTION FOR A THREE-DIMENTIONAL ELASTIC MEDIUM

The 3-D frequency domain Green's functions U_{ij} and T_{ij} for an elastic medium have the following forms

$$U_{ij} = \frac{1}{4\pi\mu}\left(\psi\delta_{ij} - \chi r_{,i}r_{,j}\right),$$

$$T_{ij} = \frac{1}{4\pi}\left[A\left(\delta_{ij}\frac{\partial r}{\partial \mathbf{n}} + r_{,j}n_i\right)\right.$$

$$\left. +B\left(n_j r_{,i} - 2r_{,i}r_{,j}\frac{\partial r}{\partial \mathbf{n}}\right) + Cr_{,j}r_{,i}\frac{\partial r}{\partial \mathbf{n}} + Dr_{,i}n_j\right] \qquad (A. 1)$$

and

$$\psi = (-\frac{C_2^2}{\omega^2 r^2} - i\frac{C_2}{\omega r} + 1)\frac{e^{-i\omega r/C_2}}{r} + \frac{C_2^2}{C_1^2}\left(\frac{C_1^2}{\omega^2 r^2} + i\frac{C_1}{\omega r}\right)\frac{e^{-i\omega r/C_1}}{r},$$

$$\chi = (-\frac{3C_2^2}{\omega^2 r^2} - i\frac{3C_2}{\omega r} + 1)\frac{e^{-i\omega r/C_2}}{r}$$

$$+\frac{C_2^2}{C_1^2}\left(\frac{3C_1^2}{\omega^2 r^2} + i\frac{3C_1}{\omega r} - 1\right)\frac{e^{-i\omega r/C_1}}{r} \qquad (A. 2)$$

where $A = d\psi/dr - \chi/r$, $B = -2\chi/r$, $C = -2d\chi/dr$, $D = \left(C_1^2/C_2^2 - 2\right)\left(d\psi/dr - d\chi/dr - 2\chi/r\right)$, μ is the shear modulus of the elastic medium, and C_1, C_2 are the compressive and shear wave velocities of the elastic medium, respectively.